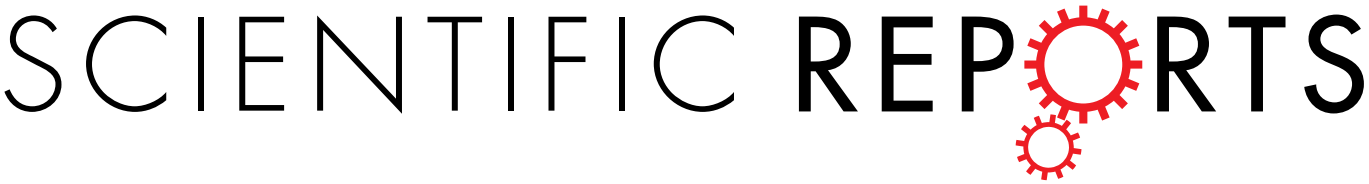

OPEN

Vascularised endosteal bone tissue in armoured sauropod dinosaurs

Anusuya Chinsamy[1], Ignacio Cerda[2] & Jaime Powell[3]

Received: 14 October 2015
Accepted: 04 April 2016
Published: 26 April 2016

The presence of well-vascularised, endosteal bone in the medullary region of long bones of nonavian dinosaurs has been invoked as being homologous to medullary bone, a specialised bone tissue formed during ovulation in birds. However, similar bone tissues can result as a pathological response in modern birds and in nonavian dinosaurs, and has also been reported in an immature nonavian dinosaur. Here we report on the occurrence of well-vascularised endosteally formed bone tissue in three skeletal elements of armoured titanosaur sauropods from the Upper Cretaceous of Argentina: i) within the medullary cavity of a metatarsal, ii) inside a pneumatic cavity of a posterior caudal vertebra, iii) in intra-trabecular spaces in an osteoderm. We show that considering the criteria of location, origin (or development), and histology, these endosteally derived tissues in the saltasaurine titanosaurs could be described as either medullary bone or pathological bone. Furthermore, we show that similar endosteally formed well-vascularised bone tissue is fairly widely distributed among nondinosaurian Archosauriformes, and are not restricted to long bones, but can occur in the axial, and dermal skeleton. We propose that independent evidence is required to verify whether vascularised endosteal bone tissues in extinct archosaurs are pathological or reproductive in nature.

Typically endosteally formed bone in vertebrates tends to be avascular lamellar or parallel-fibered bone tissue[1,2]. However, endosteally formed tissue called medullary bone, is known to occur in the medullary cavities of birds[3–10], and has been reported in nonavian dinosaurs[9,11,12]. However a similar endosteally formed tissue is also known to be pathological in extant birds[13,14]. Thus, the occurrence of well-vascularised endosteally formed bone tissue in nonavian archosaurs has been interpreted as both medullary bone[9,11,12], as well as pathological bone[15–17,19–23] (Table 1). Most of these reports are from long bones of nonavian dinosaurs, although, Reid[15] described a well-vascularised endosteally formed bone as a pathology (possibly caused by cancerous metastasis) in an internal cavity of a Wealden sauropod vertebra. Furthermore, it appears that such bone tissue occurs quite widely among non-dinosaurian archosaurs[17–19], and they have been likewise referred to as pathological, reproductive or of unknown origin[18] (Table 1). Researchers have attempted to use various criteria to distinguish medullary bone[9,11,12] from pathological bone[16] or other endosteally derived medullary bone-like tissues[18]. The problem nevertheless still persists, and appears to be fertile ground for fostering research in this area[24,25].

In the current study we describe the occurrence of well-vascularised endosteal bone tissue in an osteoderm, a vertebra and a metatarsal of armoured titanosaur sauropods from the Upper Cretaceous of Argentina. Here we propose the likely causes of its formation and the implications for the identification of endosteal tissues homologous to avian medullary bone in fossil archosaurs.

Materials and Methods

The bone histology of a metatarsal (PVL 4017–127), a distal caudal vertebra (PVL 4017–140) and an osteoderm (PVL 4017−113) of saltasaurine titanosaurs (possibly *Saltasaurus loricatus*, see supplementary information) are described here. This material forms a subset of a larger sample comprising of seventy-four bones representing various parts of the skeleton of titanosaur sauropods (Sup Table S1), including both axial and appendicular elements. The three specimens described here were collected from the Upper Cretaceous (? late Campanian–Maastrichtian) sediments of the Lecho Formation at the locality of El Brete (south of Salta Province, Argentina)[26,27], and were assigned to *Saltasaurus loricatus* on the basis of morphology and/or close association with diagnostic elements[26–28]. Nevertheless, since autapomorphic features are absent from these

[1]University of Cape Town, Department of Biological Sciences, Private Bag X3, Rhodes Gift, 7700 South Africa. [2]CONICET, Instituto de Investigación en Paleobiología y Geología, Universidad Nacional de Río Negro, Museo Carlos Ameghino, Belgrano 1700, Paraje Pichi Ruca (predio Marabunta) 8300, Cipolletti, Río Negro, Argentina. [3]CONICET, Facultad de Ciencias Naturales Universidad Nacional de Tucumán, Miguel Lillo 205, (4000) Tucumán, Argentina. Correspondence and requests for materials should be addressed to A.C. (email: anusuya.chinsamy-turan@uct.ac.za)

Taxa	Element	Endosteal Reaction	Periosteal Reaction	Cause	Ref.
Tarjadia	osteoderm	X	–	Uncertain	19
Calyptosuchus	osteoderm	X	_	Uncertain	17
Bakonydraco	mandible	X	–	Non-pathological*	18
Pterodaustro	femur	X	_	Reproductive+	58
Mussaurus	femur	X	Uncertain	Pathological	16
Allosaurus	tibia	X	X	Reproductive^	12
Allosaurus	phalanx	X	X	Pathological	20
T. rex	tibia	X	_	Pathological	21
T. rex	femur and tibia	X	_	Reprodutive	9
Wealden sauropod	vertebrae	X	–	Pathology	15
Tenontosaurus	tibia and femur	X	–	Reproductive	12
Dysalotosaurus	tibia	X	_	Reproductive	11
Transylvanian dinosaur	femur	X	X	Pathology	14
Stegosaurus	tibia	X	–	Pathology	23
Saltasaurus	vertebrae	X	–	Uncertain	#
	osteoderm	X	–	Uncertain	#
	metatarsal	X	X	Pathological	#

Table 1. Occurrence of highly vascularized endosteal bone tissue in Archosauriformes. *original authors suggest nonpathological, but current study proposes pathological. ^original authors suggest reproductive, but others (14) propose pathological. +original authors proposed possibly reproductive but were uncertain. #current study.

elements, we only refer to them as indeterminate saltasaurine titanosaurs. It is worth noting though that even if our diagnosis that they are *Saltasaurus loricatus* is incorrect, the elements are all from Saltasaurinae, and do not detract from our findings. The preparation of the histological sections was carried out in the Departamento de Geología de la Universidad Nacional de San Luis in Argentina. Thin sections were prepared using the method outlined by Chinsamy and Raath[29] (see sup Fig. S1 for location of sections) and they were studied using a petrographic polarizing microscope (Nikon E200 pol). Nomenclature and definitions of structures used in this study are derived from Francillon-Viellot *et al.*[1] and Chinsamy-Turan[2].

Results

Except for the metatarsal, caudal vertebra and osteoderm, the histology of 74 other postcranial bones of sauropod titanosaurs studied (see supplementary Table S1) did not exhibit any unusual features (i.e., vascularised endosteal bone). Thus, here we limit our report to the atypical features observed in the three bones mentioned. In the sampled metatarsal (Fig. 1a), the transverse sections obtained from the mid-shaft region shows a thin outer band of primary bone tissue (Fig. 1b,c), while the rest of compacta is extremely highly remodelled and reaches dense Haversian proportions (Fig. 1b,d). The innermost parts of the cortex has a large amount of trabeculae which tend to have thick deposits of lamellar bone and the interstitial tissue also predominantly consists of lamellar bone, although there is also some compacted coarse cancellous bone present. The medullary region exhibits a rather compacted appearance under low magnifications. In a distinct portion of the section, the cancellous bone tissue extends from the medullary cavity to the outer cortex (Fig. 1a). At level of the outer cortex of this region, a rather unusual excavation is evident and the primary bone in this region is composed of coarse bundles of mineralized fibres (Fig. 1e,f). A high degree of porosity is also evident in this area. Some distinct larger cavities are observed at the medullary region (Fig. 1g,h). These cavities show a distinctive resorptive margin, which is followed by a secondary deposition (sensu Francillon-Vieillot[1]) of a tissue intermediate between parallel-fibered and woven bone tissue with some vascular spaces entrapped within the bone matrix (Fig. 1i,j). Some of these channels have narrow bands of lamellar bone deposits. Some regions around the large cavities possess thick bands of lamellar bone tissue, which alternates with a well-vascularised region of parallel and woven-fibered bone (Fig. 1j,k). Whereas osteocyte lacunae in the parallel-fibered matrix are flattened and oriented in parallel each other, those located in the woven-fibered bone possess irregular shapes and lacks spatial organization (Fig. 1k,l). In parts of the periosteal region, there is a large amount of resorption of the original dense Haversian bone with the subsequent deposition of lamellar bone. However, the lamellar bone has different orientations, and to some extent resembles compacted coarse cancellous bone.

In the caudal vertebra, three sections were prepared (two from the middle region and one from the posterior area). All three sections of the vertebra show a thick layer of endosteal bone that lines a large pneumatic cavity (Fig. 2a). The compact bone is almost entirely composed of dense Haversian bone tissue (Fig. 2b). Remains of periosteal bone, which grades from parallel-fibered (e.g. ventral cortex) to fibrolamellar bone (e.g. lateroventral region), are observed in outermost portion of the element (Fig. 2c). An atypical endosteal tissue is observed coating the large pneumatic cavity of the vertebra. The fibrillar organization of this unusual endosteal tissue appears to be variable and ranges from lamellar to parallel-fibered to woven bone (Fig. 2d–i). Cementing lines separate the well-vascularised endosteal bone from the "normal" lamellar bone tissue (Fig. 2g–i). Osteocyte lacunae are densely grouped in some areas and they exhibit an irregular shape and a chaotic organization i.e. quite different from the pattern observed in the surrounding lamellar bone tissue (Fig. 2f,i). The tissue often includes "primary"

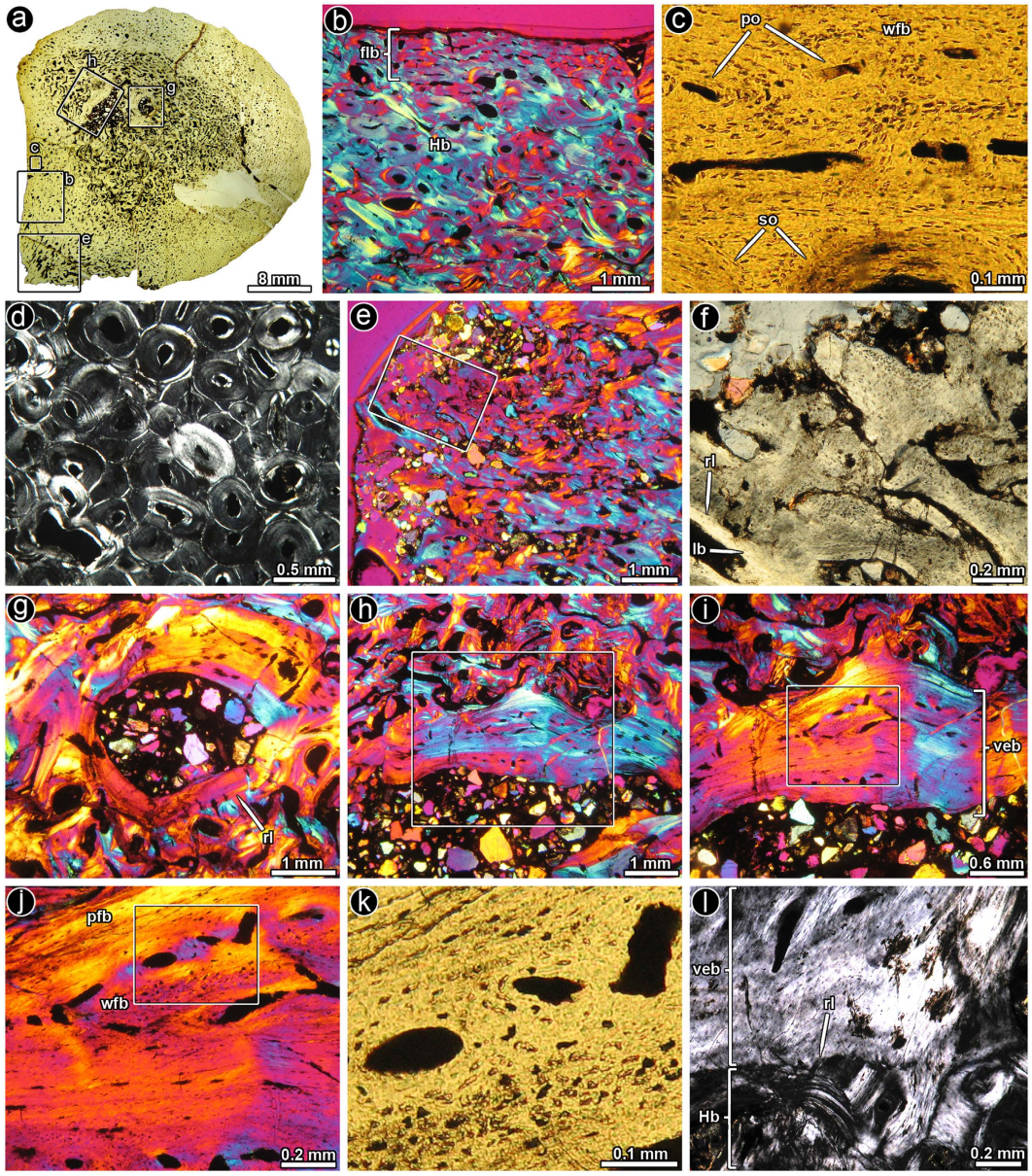

Figure 1. Bone histology of saltasaurine titanosaur metatarsal PVL 4017–127. (**a**) Complete transverse section of the metatarsal. Note the rather compacted general appearance of the bone, even in the cancellous region. The external cortex exhibits a shallow excavation in portion of the sample (left bottom margin), which also exhibits a high degree of porosity. (**b**) General view of the cortical bone, which is mostly composed of dense Haversian bone tissue. A thin layer of unremodelled primary fibro-lamellar bone is observed at the subperiosteal region. (**c**) Detail of primary fibro-lamellar bone tissue at the outer cortex. (**d**) Enlarged view of the dense Haversian bone tissue formed at the mid-cortex. (**e**) General view of the external cortex showing a highly porous tissue. (**f**) Detail of the same region showing a highly fibrous primary bone tissue and some secondary osteons. (**g**) Internal cavity in the medullary region, which is coated a thick layer of parallel and lamellar bone tissue. (**h**) General view of the medullary region in which a thick band of vascularised endosteal bone is formed around a large internal cavity. (**i**) Detail of the same region in h. Note the roughly stratified pattern of the vascularised endosteal bone tissue, with successive layers of woven- and parallel-fibered bone tissue. (**j**) Detail of the same region showing the transition between a poorly vascularised parallel-fibered bone and more vascularised woven-fibered bone in the vascularised endosteal bone. (**k**) Detailed view of the woven-fibered matrix in the vascularised endosteal bone tissue. Note the presence of well-developed primary osteons. (**l**) Detail view of the vascularised endosteal bone tissue. The resorption line between the dense Haversian bone and the vascularised endosteal bone demonstrate the secondary nature of the latter tissue. Images (**a,c,k**): normal transmitted light; (**d,l**): cross polarized light; (**f**) single plane polarized light; (**b,e,g-j**): cross polarized light with lambda compensator. Abbreviations: lb, lamellar bone; flb, fibro-lamellar bone tissue; Hb, Haversian bone; pfb, parallel-fibered bone tissue; po, primary osteons; rl, resorption line; so, secondary osteons; veb, vascularised endosteal bone; wfb, woven-fibered bone tissue.

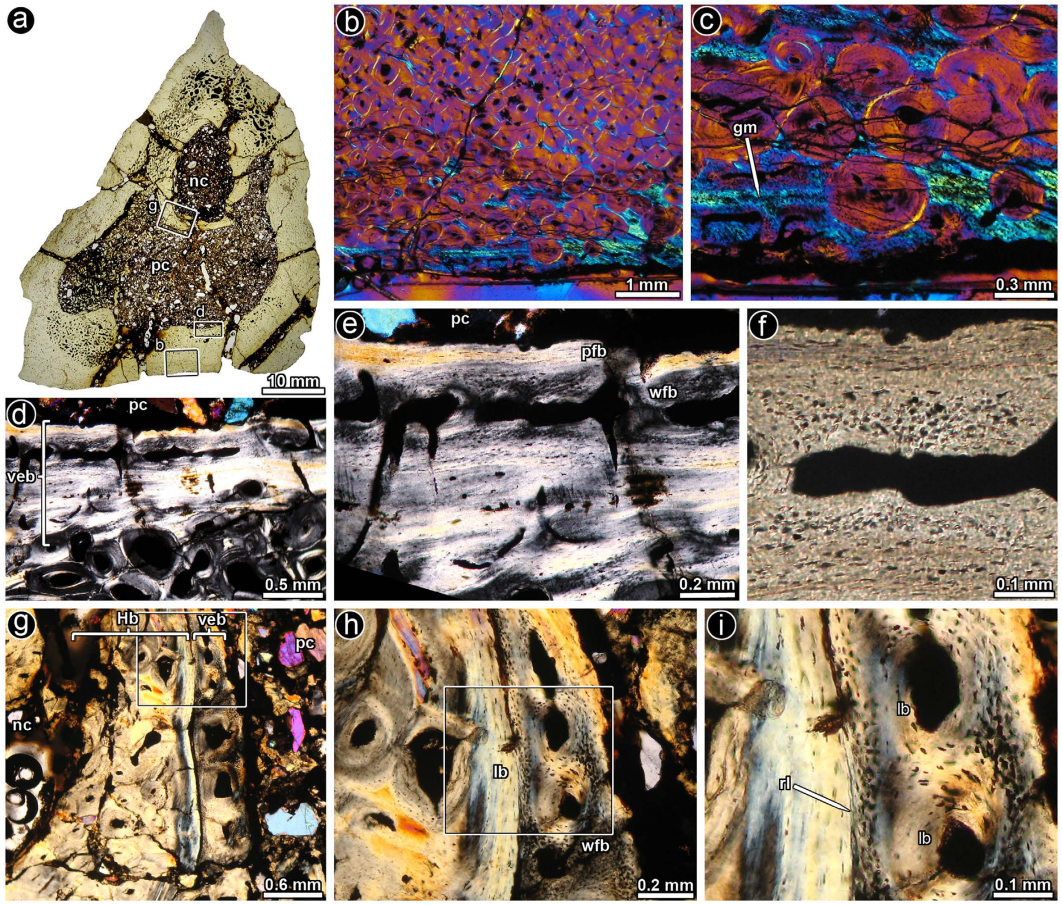

Figure 2. Bone histology of saltasaurine titanosaur distal caudal vertebra PVL 4017–140. (**a**) Complete transverse section of the vertebra. A large pneumatic cavity is formed in the centrum and part of the neural arch. (**b**) General view of the cortical bone, which is mostly composed of dense Haversian bone tissue. A thin layer of unremodelled primary bone is observed at the outer region. (**c**) Detail of primary bone tissue at the outer cortex. (**d**) General view of the inner cortex showing the bone tissue around the pneumatic cavity. Note the presence of a thick band of vascularised endosteal bone around a large internal cavity. (**e**) Detail of d. Note the stratified pattern of the vascularised endosteal bone tissue, with successive layers of woven- and parallel-fibered bone tissue. (**f**) Detail of the same picture showing the transition between a poorly vascularised parallel-fibered bone and more vascularised woven-fibered bone in the vascularised endosteal bone. Note the distinct differences in the osteocyte lacunae shape, density and arrangement. (**g**) Vascularised endosteal bone tissue and Haversian bone tissue below the neural canal. (**h**) Detail of g showing the transition between dense Haversian bone and vascularised endosteal bone. (**i**) Detail of h. The resorption line between the dense Haversian bone and the vascularised endosteal bone demonstrate the secondary nature of the latter tissue. Images (**a**,**f**): normal transmitted light; (**b**,**c**), polarized light with lambda compensator; (**d**,**e**,**g**-**i**): cross polarized light. Abbreviations: lb, lamellar bone; gm, growth mark; Hb, Haversian bone; nc: neural canal; pc, pneumatic cavity; pfb, parallel-fibered bone tissue; rl, resorption line; veb, vascularised endosteal bone; wfb, woven-fibered bone tissue.

osteons, i.e. vascular channels surrounded by centripetally deposited lamellar bone tissue, as well as some channels showing obvious resorptive surfaces.

The sampled osteoderm is a conical plate for which a histological description was published by Cerda and Powell[28]. The thin sections obtained from the osteoderm reveal that the overall structure is rather cancellous (as opposed to being compact), with abundant inter-trabecular spaces lined by lamellar bone (Fig. 3a,b). Remains of primary bone tissue are preserved in some areas and consist of coarsely bundled mineralized structural fibers (Fig. 3c), which have been commonly observed in osteoderms of titanosaurs and ankylosaurs and originate from metaplasic ossification[23,28,30,31]. Dense Haversian bone is formed at the internal and lateral cortices (Fig. 3d). Large internal cavities are located near the deep cortex (Fig. 3e–g). Some of these cavities are lined with a highly vascularised secondary bone tissue (Fig. 3f–h). This unusual endosteal bone is distinct from the secondary lamellar bone formed in the cancellous bone and consists of parallel-fibered and woven bone tissue. The secondary nature of this endosteal bone is clearly revealed by the resorptive surface of the "normal" secondary lamellar bone from which the vascularised endosteal tissue is deposited (Fig. 3f). Osteocyte lacunae are densely grouped together and

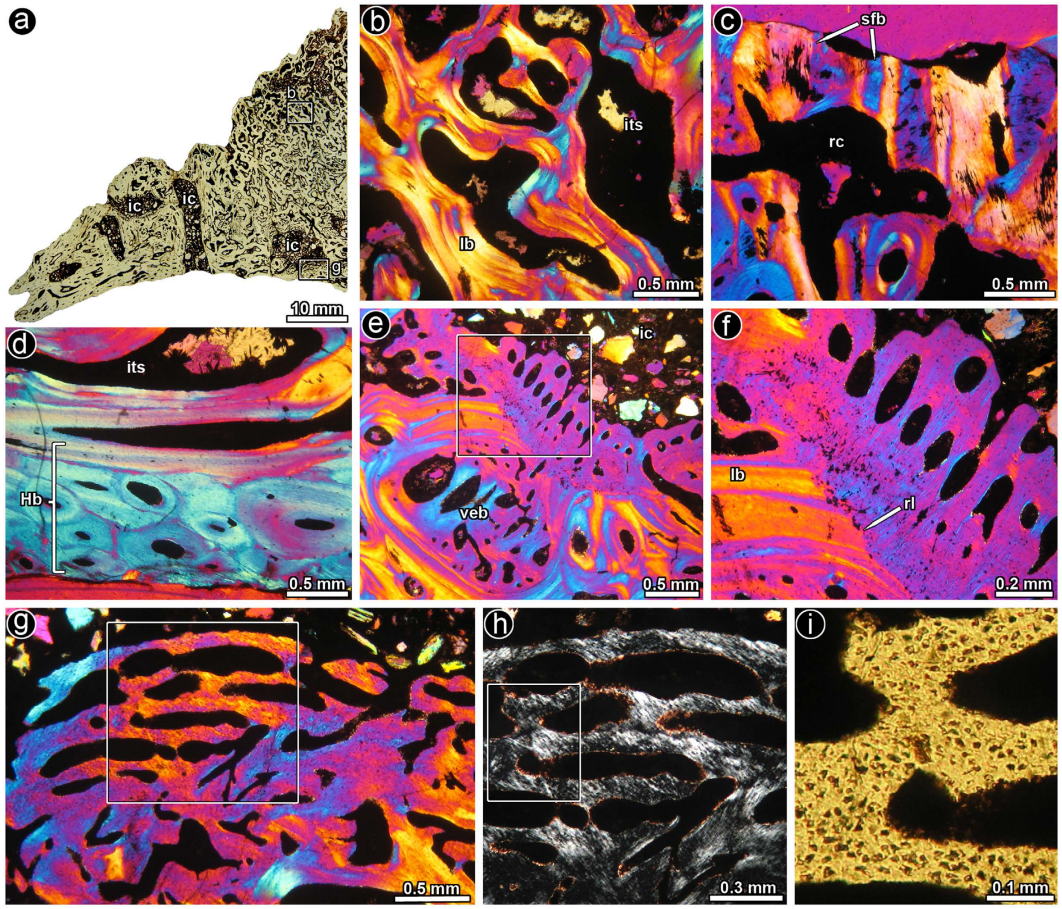

Figure 3. Bone histology of saltasaurine titanosaur osteoderm PVL 4017–113. (**a**) Half portion of the osteoderm in transverse section. The internal microanatomy of the elements is characterized by abundant cancellous bone and several large internal cavities. (**b**) Detailed view of the secondary cancellous bone tissue, which is entirely formed by secondary lamellar bone tissue deposited during different episodes of remodeling. (**c**) Remains of primary bone tissue at the outer cortex, which is formed by interwoven bundles of mineralized structural fibres (**d**) Enlarged view of the dense Haversian bone tissue formed at the internal cortex of the osteoderm. (**e**) General view of the inner cortex showing the bone tissue around the internal cavity. Note the presence of a thick band of vascularised endosteal bone is formed around a large internal cavity. (**e**) Highly vascularised endosteal bone is formed around a large internal cavity. Note that an adjacent resorption cavity has been also filled with vascularised endosteal bone. (**i**) Detail of e showing the abrupt transition between endosteal lamellar bone tissue and vascularised endosteal tissue. A distinctive resorption line demarcates this transition. (**g**) Highly vascularised endosteal bone is formed around a large internal cavity. (**h**) Detail of g showing the arrangement of intrinsic fibres. (**i**) Detailed view of the same picture showing the shape, density and arrangement of osteocyte lacunae in the vascularised endosteal bone. Images (**a**,**i**): normal transmitted light; (**b**–**l**): cross polarized light with lambda compensator; (**h**) polarized light. Abbreviations: lb, lamellar bone; Hb, Haversian bone; rc, resorption cavity; rl, resorption line; ic, internal cavity; its, intertrabecular spaces; veb, vascularised endosteal bone.

they exhibit globular to rounded shapes (Fig. 3i). Several inter-trabecular spaces located near the large cavities are also infilled with this unusual secondary bone tissue (Fig. 3e).

Discussion

In the current study we were able to identify at least three ways in which the endosteal bone formed: i) The typical or most common type of endosteal bone tissue observed among many vertebrates and the saltasaurine specimens studied here is an avascular lamellar lining bone tissue[1,2] (Supplementary Fig. S2–S6). ii) The second type of endosteal bone appears to be an extensively developed bone tissue consisting of vascularised lamellar/parallel-fibered and woven-fibered bone, and can sometimes alternate to form a stratified pattern (Fig. 2e). This tissue was observed mainly in the pneumatic cavities of the saltasaurine caudal vertebra and locally in the medullary cavity of the metatarsal. iii) The third type of endosteal bone tissue consisted of a highly vascularised parallel-fibered and coarsely fibered woven bone tissue. This is predominantly seen in the cancellous spaces and large channels in the osteoderm (Fig. 3e,g). In previous histological studies on dermal, axial and appendicular bones of titanosaur sauropods[28,32–42] only the first type of endosteal bone tissues were reported, and no mention

was made of the other endosteal tissue types. Furthermore, in our sample of 74 bones of titanosaurs we only found the second and third types of endosteally formed tissue in three bones. In addition, they have also not been reported in previous studies of more than 200 bones of other titanosaur sauropods studied histologically. These findings suggest that these endosteal tissue types are not common in the skeleton of titanosaurs, and they appear to be unrelated to cortical drift or biomechanical adaptive remodelling. However, it is interesting that similar vascularised endosteal tissues are known to occur among extant vertebrates under particular circumstances, i.e. in reproductively active avian females[4,8] and under some pathological conditions[13,14].

Among extant archosaurs, reproduction inflicts particular histological changes in the bone microstructure of females. In crocodiles, long bones and osteoderms of females (as opposed to males) are extensively reconstructed during egg laying due to resorption of calcium for the calcification of eggshells[43–46]. Breeding females of *Crocodylus niloticus*[46], *Alligator mississipiensis*[47] and *Crocodylus johnstoni*[48] are reported to show extensive remodelling of their osteoderms, which often result in the obliteration of skeletal growth marks. On the other hand, among several extant bird taxa, prior to egg production females deposit a specially formed bone tissue (called medullary bone) within the medullary cavity of various bones in the skeleton, which acts as a reservoir for calcium during egg shelling[4,8,9].

Four nonavian dinosaur taxa are reported to have a reproductive bone tissue homologous to that of avian medullary bone (Table 1). The identification of these tissues as medullary bone in these nonavian dinosaurs has been on the basis of location (within medullary cavities of long bones), origin (i.e. endosteally developed), and histology (vascularised woven bone tissue with its characteristic birefringence). Considering these criteria, it appears that the endosteally formed vascularised bone tissue formed in the saltasaurines described here could be medullary bone. However, these same criteria (location, origin and histology) also hold true for pathological bone. One of the diagnostic characteristics generally used to identify medullary bone in fossil taxa is its location within the medullary cavities of long bones. However, although medullary bone is predominantly located in long bones, it can also occur in various bones of the skeleton, including axial, and distal appendicular bones, as well as in pneumatic bones[49]. This means that the location of well-vascularised endosteal bone tissue within the vertebra and metatarsal of our study material could easily also fit the criteria for medullary bone. Our observation of this unusual bone tissue within the pneumatic cavity of the caudal vertebra, does not preclude it from being medullary bone since such bone has been located within pneumatic bones of birds[49]. However, pathological bone can also be found in any part of the skeleton and within medullary cavities. Thus, on the basis of location, our findings of highly vascularised endosteal bone tissue in the saltasaurine titanosaur bones could be interpreted as a pathology as well[16]. Considering the origin criteria, medullary bone develops from the endosteum of medullary cavities and other internal spaces and is under hormonal control in reproductive females[50]. It is not associated with any specialized periosteal bone tissue. Vascularised endosteally formed tissue is also produced as a result of a pathology e.g. avian osteopetrosis[10,16,22] and during fracture healing processes[20]. Avian osteopetrosis often results in both a periosteal and an endosteal reaction, although there are reports of only endosteal reactive bone tissue being formed[13]. In the case of our samples, none of the bones show any signs of an external callus, and in addition, although the metatarsal shows some unusual histology in a localized periosteal part of the cortex, a distinctive periosteal reactive bone tissue is not observed. Other diseases, e.g., Paget's disease, osteomyelitis, lytic metastatic lesions from cancers can also cause osteoblastic activity that can result in pathologically formed endosteal bone tissues[51–54]. Given that both medullary bone and various pathologies can result in well-vascularised endosteal bone tissue we cannot conclusively identify whether the tissues in the saltasaurine titanosaur vertebra and the osteoderm are homologous to medullary bone or whether they are pathological. The unusual histology of the metatarsal is also endosteally formed but in this case, it could be diagnosed as a pathological response (see below). Finally, taking into account the third criterion (histology), medullary bone has been characterized as a well-vascularised endosteally formed woven bone tissue[2,9]. Pathological bone on the other hand, can manifest as different kinds of bone tissue: for example, several diseases can result in well-vascularised woven bone tissue (e.g. metastatic cancer and osteomyelitis), and in diseases such as avian osteopetrosis the bone tissue is characterized by a high density of osteocyte lacunae, whilst Paget's diseases is distinctive in having mainly remodelled lamellar kind of bone tissue[48]. In our saltasaurine titanosaur samples, the histological nature of the tissue rules out avian osteopetrosis and Paget's disease. In addition, the lack of any fracture callus excludes fracture healing as the cause of the deposition. However, other diseases such as, osteomyelitis and metastatic cancer could have resulted in such anomalous endosteally formed vascularised bone tissue[55].

Besides location, origin and histology, attainment of sexual maturity[11,12,18] has also been used as an additional criterion for identification of medullary bone (since it is only formed in reproductively active females). The periosteal bone tissue of the saltasaurine titanosaur metatarsal and the caudal vertebra suggests that they were from still rapidly growing individuals which had not experienced a "slow down" in growth generally attributable to the attainment of sexual maturity.

Another interesting feature of the saltasaurine endosteally formed bone tissue is that unlike medullary bone, besides the well-vascularised endosteal woven bone, it also has a large amount of endosteally formed parallel-fibered and lamellar bone tissues which sometimes appear to be formed in cycles (Figs 1I and 2e). In some instances, such as in the vertebrae and the metatarsal, this tissue can result in a thick layer (Figs 1g and 3g) and leads to some compaction of the element. Therefore, "cyclically" formed endosteal bone in the vertebra and in the metatarsal could also be seen as being different to medullary bone usually described in the literature[2,9].

Besides the presence of an abnormal endosteal bone tissue, the metatarsal exhibits two particular features that are possibly linked to the development of the vascularised endosteal bone. As previously described, the cancellous bone of the metatarsal reaches the outer cortex in particular region of the element, which is also characterized by the presence of a distinct excavation (Fig. 1a). The preserved primary bone tissue of this area is also distinctive in being composed of coarse bundles of mineralized fibres. These characteristics suggest a possible pathological origin of this tissue, and it is therefore likely that the vascularised endosteal tissue in the metatarsal is pathological.

The presence of vascularised endosteal bone tissue in the saltasaurine osteoderm poses an enigma. Indeed such tissue has been observed in osteoderms of fossil Archosauriformes. Scheyer *et al.*[17] described pockets of convoluted well-vascularised secondary bone within an osteoderm of the aetosaur, *Calyptosuchus wellesi*, and Cerda *et al.*[19] described endosteally formed bony trabeculae consisting of woven- and parallel-fibered bone within a cavity of an osteoderm of the doswelliid, *Tarjadia*. Several authors have proposed that the large cavities located within titanosaur osteoderms are suggestive of their role in calcium mobilization[20,33,38]. However, although crocodiles utilize calcium from their osteoderms they do not first deposit a special tissue (such as the high vacularised endosteal tissue of medullary bone), which is then mobilized. They appear to use the existing bone within the osteoderms, which result in the extensive remodelling of the osteoderms (as has been noted by several researchers).

Recently Prondvai and Stein[18] described a "medullary-like" bone tissue in the mandibles of an azdarchid pterosaur (*Bakonydraco galaczi*). These researchers suggested the possibility that the tissue could be non-pathological since it occurs in four out of seven mandibles of the pterosaur, and they further suggested that it is not in response to reproduction since three of the specimens are fast growing immature individuals. However, given that outbreaks of disease are known to affect several individuals of wild populations[56], it is possible that this tissue could reflect a pathological response in the four individuals. This tissue[18] appears to resemble the vascularised endosteal bone tissue we describe in the saltasaurine titanosaur osteoderm and vertebra.

Our data suggests that only in the metatarsal can we deduce with independent evidence that the endosteal bone tissue is formed as a result of pathology. Vascularised endosteal bone tissue has been recorded and interpreted as being pathological in osteoderms of other Archosauriformes[17,19]. A similar tissue was described by Reid[15] as a pathology in a pneumatic cavity of a sauropod vertebrae. Given that these previous studies have not provided any independent evidence for these being pathological, we cannot use them in support of a pathological origin for the observations made in our specimens. However, the finding of such endosteal bone tissue in our specimens, and possibly in the *Bakonydraco*[18] suggests that such bone tissues appears to be fairly widespread within the phylogeny of Archosauriformes.

In conclusion, our study shows that the main criteria for the identification of medullary bone in fossil taxa i.e. location, origin, histology (including extent of mineralisation and birefringence patterns), cannot be employed because they also fit for different types of pathologies. For this reason, independent evidence is needed to assert either a pathological and/or reproductive origin for the occurrence of well-vascularised endosteal bone tissues. For example such evidence to support a pathological origin, could be corresponding periosteal reactive bone[14,16], and/or lack of sexual maturity[21], whereas independent evidence to support medullary bone could be morphometric studies[57] or other evidence to support the identification of females[10], or presence of eggs in the oviduct[2]. In the saltasaurine titanosaur samples studied here, direct independent evidence for a pathological cause of the well-vascularised endosteal bone tissue is only evident for the metatarsal. Interestingly in all the previous reports of vascularised endosteal tissue (Table 1), independent evidence besides the location, origin and histology has also only been provided in those specimens for which a pathological hypothesis is supported. To date, there is no independent evidence to support the presence of a tissue homologous to avian medullary bone in nonavian archosaurs.

References

1. Francillon-Vieillot, H. *et al.* In *Skeletal biomineralisation: patterns, processes and evolutionary trends* (ed. Carter, J. G.) 471–530 (Van Nostrand Reinhold, 1990).
2. Chinsamy-Turan, A. *The Microstructure of Dinosaur Bone: Deciphering Biology with Fine Scale Techniques.* (Johns Hopkins University Press, 2005).
3. Bloom M. A., Domm L. V., Nalbandov A. X. & Bloom W. Medullary bone of laying chickens. *Am. J. Anat.* **102,** 411–451 (1958).
4. Simkiss K. *Calcium Reproductive Physiology*. (Chapman and Hall, 1967).
5. Rick, A. M. Bird medullary bone: a seasonal dating technique for faunal analysis. *Can. Archaeol. Ass.* **7,** 180–190 (1975).
6. Miller, S. C. & Bowman, B. M. Medullary bone osteogenesis following estrogen administration to mature male Japanese quail. *Dev. Biol.* **87,** 52–63 (1981).
7. Schraer, H. & Hunter, S. J. The development of medullary bone: A model for osteogenesis. *Comp. Biochem. Physiol.* **82,** 13–17 (1985).
8. Dacke, C. G. *et al.* Medullary bone and avian calcium regulation. *J. Exp. Biol.* **184,** 63–88 (1993).
9. Schweitzer, M. H., Wittemeyer, J. L. & Horner, J. R. Gender-specific reproductive tissue in ratites and *Tyrannosaurus rex*. *Science* **380,** 1456–1460 (2005).
10. Chinsamy, A., Chiappe, L., Marugan-Lobon, J., Chunling, G. & Fengjiao, Z. Gender identification of the Mesozoic bird *Confuciusornis sanctus*. *Nat. Comm.* **4,** doi: 10.1038/ncomms2377 (2013).
11. Hübner, T. R. Bone histology in *Dysalotosaurus lettowvorbecki* (Ornithischia: Iguanodontia) - variation, growth, and implications. *PLoS One* **7,** e29958 (2012).
12. Lee, A. H. & Werning, S. Sexual maturity in growing dinosaurs does not fit reptilian growth models. *Proc. Natl. Acad. Sci. USA* **105,** 582–587 (2008).
13. Holmes, J. R. Experimental transmission of avian osteopetrosis. *J. Comp. Pathol.* **68,** 439–451 (1958).
14. Chinsamy, A. & Tumarkin-Deratzian, A. Pathological bone tissue in a turkey vulture and a nonavian dinosaur. *Anat. Rec.* **292,** 1478–1484 (2009).
15. Reid, R. E. H. Bone histology of the Cleveland-Lloyd dinosaurs and of dinosaurs in general, part I: Introduction: Introduction to bone tissues. *Brigham Young U. Geol. Stud.* **41,** 25–71 (1996).
16. Cerda, A., Chinsamy, A. & Pol. D. Unusual endosteally formed bone tissue in a Patagonian basal sauropodomorph Dinosaur. *Anat. Rec.* **297,** 1385–1391 (2014).
17. Scheyer, T. M., Desojo, J. B. & Cerda, I. A. Bone histology of phytosaur, aetosaur, and other archosauriform osteoderms (Eureptilia, Archosauromorpha). *Anat. Rec.* **297,** 240–260 (2014).
18. Prondvai, E. & Stein, K. H. W. Medullary bone-like tissue in the mandibular symphyses of a pterosaur suggests non-reproductive significance. *Sci. Rep.* **4,** doi: 10.1038/srep06253 (2014).
19. Cerda, I. A., Desojo, J. B., Trotteyn, M. J. & Scheyer, T. M. Osteoderm histology of Proterochampsia and Doswelliidae (Reptilia: Archosauriformes) and their evolutionary and paleobiological implications. *J. Morphol.* **276,** 385–402. doi: 10.1002/jmor.20348 (2015).

20. Annè, J. *et al.* Synchrotron imaging reveals bone healing and remodelling strategies in extinct and extant vertebrates. *J. R. Soc. Interface* **11,** 20140277, doi: 10.1098/rsif.2014.0277 (2014).
21. Tremaine, K., Woodward Ballard, H. & Horner, J. Bone histology of an immature *Tyrannosaurus rex* with comments on unusual endosteal bone tissue. *J. Vert. Palaeontol.* 74th Annual Meeting Abstract Book, Berlin, Germany, page 240 (2014).
22. Redelstorff, R., Hayashi, S., Rothschild, B. M. & Chinsamy, A. Non-traumatic bone infection in stegosaurs from Como. *Lethaia* doi: 10.1111/let.12086 (2014).
23. Cerda, I. A., Desojo, J. B., Trotteyn, M. J. & Scheyer, T. M. Osteoderm histology of Proterochampsia and Doswelliidae (Reptilia: Archosauriformes) and their evolutionary and paleobiological implications. *J. Morphol.* **276,** 385–402. doi: 10.1002/jmor.20348 (2015).
24. Chinsamy, A., Cerda, I. & Powell, J. Unusual Endosteal bone tissue in *Saltasaurus loricatus* (Dinosauria:Sauropoda). Abstracts volume of the 3rd International Symposium on Paleohistology, Bonn, Germany, page 56 (2015).
25. Werning, S., Schweitzer, M. H. & Padian, K. When microstructure isn't enough: Additional diagnostic criteria to test among hypotheses of bone tissue identity. *J. Vert. Palaeontol*. 75th Annual Meeting Abstract Book, Dallas, Texas, page 235 (2015).
26. Bonaparte, J. F. & Powell, J. E. A continental assemblage of tetrapods from the Upper Cretaceous beds of El Brete, northwestern Argentina (Sauropoda–Coelurosauria–Carnosauria–Aves). Mém. de la Soc. Géol. de France **139,** 19–28 (1980).
27. Powell, J. E. Revision of South American titanosaurid dinosaurs: Palaeobiological, palaeobiogeographical and phylogenetic aspects. *Rec. Victoria Mus*. **111,** 1–173 (2003).
28. Cerda, I. A. & Powell, J. E. Dermal armor histology of *Saltasaurus loricatus*, an Upper Cretaceous sauropod dinosaur from Northwest Argentina. *Acta Palaeont. Pol*. **55,** 389–398 (2010).
29. Chinsamy, A. & Raath, M. A. Preparation of fossil bone for histological examination. *Palaeont. afri*. **29,** 39–44 (1992).
30. Scheyer, T. M. & Sander, P. M. Histology of ankylosaur osteoderms: Implications for systematics and function *J. Vert. Paleontol*. **24,** 874–893 (2004).
31. Hayashi, S., Carpenter, K. & Suzuki, D. Different growth pattern between the skeleton and osteoderms of *Stegosaurus* (Ornithischia: Thyreophora). *J. Vert. Paleont*. **29,** 123–131 (2009).
32. Sander, M. Long bone histology of the Tendaguru sauropods: Implications for growth and biology. *Paleobiol*. **26,** 466–488 (2000).
33. Salgado, L. *Evolución y Paleobiología de los saurópodos Titanosauridae.* Doctoral thesis, Universidad Nacional de La Plata, 300 pages (2000).
34. Klein, N., Sander, M. & Suteethorn, V. Bone histology and its implications for the life history and growth of the Early Cretaceous titanosaur *Phuwiangosaurus sirindhornae*. *Geol. Soc. London, Spec. Pub*. **315,** 217–228, doi: 10.1144/SP315.15 (2009).
35. Woodward, H. N. & Lehman, T. M. Bone histology and microanatomy of *Alamosaurus sanjuanensis* (Sauropoda: Titanosauria) from the Maastrichtian of Big Bend National Park, Texas. *J. Vert. Paleontol*. **29,** 807–821 (2009).
36. Stein, K. *et al.* Small body size and extreme cortical bone remodeling indicate dwarfism in *Magyarosaurus dacus* (Sauropoda: Titanosauria). *Proc. Nat. Acad. Sci., USA* **107,** 9258–9263 (2010).
37. Company, J. Bone histology of the titanosaur *Lirainosaurus astibiae* (Dinosauria: Sauropoda) from the Latest Cretaceous of Spain. *Naturwissenschaften* **98,** 67–78 (2011).
38. Curry Rogers, K., D'Emic, M. Rogers, R., Vickaryous, M. & Cagan, A. Sauropod dinosaur osteoderms from the Late Cretaceous of Madagascar. *Nat. Comm*. **564,** doi: 10.1038/ncomms1578. (2011).
39. Gallina, P. A. Histología ósea del titinosaurio *Bonitasaura salgadoi* (Dinossauria: Sauropod) del Cretáccico superior de Patagonia. *Ameghinian* **49,** 289–302 ISSN 0002-7014 (2012).
40. Klein, N. *et al.* Modified laminar bone in *Ampelosaurus atacis* and other titanosaurs (Sauropoda): Implications for life history and physiology. *PLoS One* **7,** e36907 (2012).
41. Lacovara, K. J. *et al.* A gigantic, exceptionally complete titanosaurian sauropod dinosaur from southern Patagonia, Argentina. *Sci. Rep*. **4,** doi: 10.1038/srep06196 (2014).
42. Sellés, A. G., Marmi, J., Llácer, S. & Blanco, A. The youngest sauropod evidence in Europe. *Hist. Biol.* doi: 10.1080/08912963.2015.1059834 (2015).
43. Elsey, R. M. & Wink, C. S. The effects of estradiol on plasma calcium and femoral bone structure in alligators (*Alligator mississippiensis*). *Comp. Biochem. Physiol*. **84,** 107–110 (1986).
44. Wink, C. S., Elsey, R. M. & Mill, E. M. Changes in femoral robusticity and porosity during the reproductive cycle of the female alligator (*Alligator mississippiensis*). *J. Morphol.* **193,** 317–321 (1987).
45. Schweitzer, M. H., Elsey, R. M., Dacke, C. G., Horner, J. R. & Lamm, E.-T. Do egg-laying crocodilian (*Alligator mississipiensis*) archosaurs form medullary bone? *Bone* **40,** 1152–1158 (2007).
46. Hutton, J. M. Age determination of living Nile crocodiles from the cortical stratification of bone. *Copeia* **2,** 332–341 (1986).
47. Klein, N., Scheyer, T. & Tütken, T. Skeletochronology and isotopic analysis of a captive individual of *Alligator mississippiensis* Daudin, 1802. *Foss. Rec.* **12,** 121–131 (2009).
48. Tucker, A. Validation of skeletochronology to determine age of freshwater crocodiles (*Crocodylus johnstoni*). *Mar. Freshwater Res.* **48,** 343–351 (1997).
49. Taylor, T. G. & Moore, J. H. Avian medullary bone. *Nature* **172,** 504–505 (1953).
50. Wilson, S. & Thorpe, B. H. Estrogen and cancellous bone loss in the fowl. *Calcif. Tiss. Int*. **62,** 506–511 (1998).
51. Aoki, J. *et al.* Reactive endosteal bone formation. *Radiology* **16,** 545–555 (1987).
52. Hipp, J. A., McBroom, R. J., Cheal, E. J. & Hayes, W. C. Structural consequences of endosteal metastatic lesions in long bones. *J. Orthopaed. Res.* **7,** 82lL837 (1989).
53. Mundy. G. R. Metastasis to bone: Causes, consequences and therapeutic opportunities *Nature* **2,** 584–593 (2002).
54. Thudi, N. K. *et al.* Dickkopf-1 (DKK-1) stimulated prostate cancer growth and metastasis and inhibited bone Formation in osteoblastic bone metastases. *Prostate* **71,** 615–625 (2011).
55. Baltensperger, M. *et al.* Is primary chronic osteomyelitis a uniform disease? Proposal of a classification based on a retrospective analysis of patients treated in the past 30 years. *J. Cranio. Maxill. Surg.* **32,** 43–50 (2004).
56. Loh, R. *et al.* The pathology of devil facial tumor disease (DFTD) in Tasmanian devils (*Sarcophilus harrisii*). *Vet. Pathol.* **43,** 890–895 (2006).
57. Handley, W. D., Chinsamy, A., Yates, A. & Worthy, T. H. Sexual dimorphism in the late Miocene Mihirung *Dromornis stirtoni* (Aves: Dromornithidae) from the Alcoota Local Fauna of central Australia. *J. Vert. Paleont.* (in press).
58. Chinsamy, A., Cordoniu,L. & Chiappe, L. Palaeobiological implications of the bone histology of *Pterodaustro guinazui*. *Anat. Rec.* **292,** 1462–1477. (2009).

Author Contributions

A.C. and I.C. did the histological descriptions together, and wrote the paper. J.P. was involved in the excavation of the fossil material, and in the morphological study of the specimens. All authors reviewed the manuscript before submission.

Additional Information

Supplementary information accompanies this paper at http://www.nature.com/srep

Competing financial interests: The authors declare no competing financial interests.

How to cite this article: Chinsamy, A. *et al.* Vascularised endosteal bone tissue in armoured sauropod dinosaurs. *Sci. Rep.* **6**, 24858; doi: 10.1038/srep24858 (2016).

Vascularised endosteal bone tissue in armoured sauropod dinosaurs.

ANUSUYA CHINSAMY[1], IGNACIO CERDA[2] AND JAIME POWELL[3]

1 University of Cape Town, Department of Biological Sciences, Private Bag X3, Rhodes Gift, 7700 South Africa. Anusuya.chinsamy-turan@uct.ac.za

2 CONICET, Instituto de Investigación en Paleobiología y Geología, Universidad Nacional de Río Negro, Museo Carlos Ameghino, Belgrano 1700, Paraje Pichi Ruca (predio Marabunta) 8300, Cipolletti, Río Negro, Argentina, nachocerda6@yahoo.com.ar

3 CONICET, Facultad de Ciencias Naturales Universidad Nacional de Tucumán, Miguel Lillo 205, (4000) Tucumán, Argentina.

powell.jaime@gmail.com

SUPPLEMENTARY INFORMATION

Supplementary Table S1: list of all elements sectioned and analyzed in this study.

Taxa	Element	Collection number	Type of endosteal bone
Saltasaurus	Humerus	PVL 4017-65	Lamellar
Saltasaurus	Humerus	PVL 4017-62	Lamellar
Saltasaurus	Humerus	PVL 4017-71	Lamellar
Saltasaurus	Radius	PVL 4017-151	Lamellar
Saltasaurus	Ulna	PVL 4017-75	Lamellar
Saltasaurus	Ulna	PVL 4017-189	Lamellar
Saltasaurus	Ulna	PVL 4017-219	Lamellar
Saltasaurus	Scapula	PVL 4017-157	Lamellar
Saltasaurus	Scapula	PVL 4017-153	Lamellar
Saltasaurus	Sternal plate	PVL 4017-111	Lamellar
Saltasaurus	Femur	PVL 4017-82	Lamellar
Saltasaurus	Tibia	PVL 4017-220	Lamellar
Saltasaurus	Tibia	PVL 4017-216	Lamellar
Saltasaurus	Fibula	PVL 4017-91	Lamellar
Saltasaurus	Metatarsal	PVL 4017-127	Lamellar bone; vascularised woven fibered and parallel-fibered bone
Saltasaurus	Ilium	PVL 4017-221	Lamellar
Saltasaurus	Ilium	PVL 4017-155	Lamellar
Saltasaurus	Pubis	PVL 4017-103	Lamellar
Saltasaurus	Pubis	PVL 4017-222	Lamellar
Saltasaurus	Ischium	PVL 4017-223	Lamellar
Saltasaurus	Ischium	PVL 4017-158	Lamellar
Saltasaurus	Ischium	PVL 4017-224	Lamellar
Saltasaurus	Dorsal rib	PVL 4017-148	Lamellar
Saltasaurus	Dorsal rib	PVL 4017-146	Lamellar

Saltasaurus	Dorsal rib	PVL 4017-144	Lamellar
Saltasaurus	Dorsal rib	PVL 4017-171	Lamellar
Saltasaurus	Dorsal rib	PVL 4017-143	Lamellar
Saltasaurus	Dorsal rib	PVL 4017-225	Lamellar
Saltasaurus	Dorsal rib	PVL 4017-226	Lamellar
Saltasaurus	Posterior caudal vertebra	PVL 4017-140	Lamellar bone; Vascularised woven fibered and paralll fibered bone
Saltasaurus	Posterior caudal vertebra	PVL 4017-207	Lamellar
Saltasaurus	Mid caudal vertebra	PVL 4017-56	Lamellar
Saltasaurus	Cervical vertebra	PVL 4017-217	Lamellar
Saltasaurus	Mid caudal vertebra	PVL 4017-192	Lamellar
Saltasaurus	Osteoderm	PVL 4017-113	Lamellar bone; Vascularised woven fibered and parallel fibered bone
Lithostrotia indet.	Osteoderm	MCS-Pv 181	Lamellar
Lithostrotia indet.	Osteoderm	MCS-Pv 182	Lamellar
Lithostrotia indet.	Osteoderm	MCS-Pv 62	Lamellar
Lithostrotia indet.	Osteoderm	MPCA-Pv 67	Lamellar
Lithostrotia indet.	Osteoderm	MPCA-Pv sn	Lamellar
Neuquensaurus	Humerus	MLP CS 1009	Lamellar
Neuquensaurus	Ulna	MLP CS 1094	Lamellar
Neuquensaurus	Scapula	MLP CS 1129	Lamellar

Neuquensaurus	Femur	MCS-Pv 5/28	Lamellar
Neuquensaurus	Tibia	MPCA-Pv CS 002	Lamellar
Neuquensaurus	Tibia	MLP CS 1093	Lamellar
Neuquensaurus	Tibia	MLP CS 1303	Lamellar
Neuquensaurus	Metatarsal	MCS-Pv 174/11	Lamellar
Neuquensaurus	Ilium	MLP-CS 1056	Lamellar
Neuquensaurus	Ischium	MPCA-CS 001	Lamellar
Neuquensaurus	Dorsal rib	MCS-Pv 5/36	Lamellar
Neuquensaurus	Dorsal rib	MCS-Pv 5/37	Lamellar
Neuquensaurus	Dorsal rib	MCS-Pv 174/12	Lamellar
Neuquensaurus	Caudal vertebra	MPCA-Pv sn	Lamellar
Neuquensaurus	Caudal vertebra	MCS-Pv 180	Lamellar
Neuquensaurus	Caudal vertebra	MPCA-Pv Cs 003	Lamellar
Neuquensaurus	Caudal vertebra	MPCA-Pv Cs 006	Lamellar
Neuquensaurus	Caudal vertebra	MPCA-Pv Cs 004	Lamellar
Neuquensaurus	Caudal vertebra	MCS-Pv 174/13	Lamellar
Neuquensaurus	Caudal vertebra	MPVA-Pv Cs 005	Lamellar
Neuquensaurus	Chevron	MCS-Pv 5/32	Lamellar
Neuquensaurus	Chevron	MLP CS 1245	Lamellar
Andesaurus	Femur	MUCPv 132	Lamellar
Andesaurus	Dorsal rib	MUCPv 132	Lamellar
Andesaurus	Dorsal rib	MUCPv 132	Lamellar
Argentinosaurus	Dorsal rib	PVPH-1	Lamellar
Laplatasaurus	Fibula	MUCPv 239	Lamellar
Laplatasaurus	Metacarpal	MUCPv 239	Lamellar
Laplatasaurus	Ilium	MUCPv 239	Lamellar
Aeolosaurus sp.	Femur	MPCA-Pv 27100	Lamellar

Aeolosaurus sp.	Sternal plate	MPCA-Pv 27100	Lamellar
Aeolosaurus sp.	Dorsal rib	MPCA-Pv 27100	Lamellar
Aeolosaurus sp.	Ulna	MPCA-Pv sn	Lamellar
Aeolosaurus sp.	Mid caudal vertebra	MPCA-Pv sn	Lamellar

Institutional Abreviations: MCF-PVPH, Vertebrate Paleontology of Museo Carmen Funes, Plaza Huincul, Argentina; MCS-Pv, Vertebrate Paleontology of Museo de Cinco Saltos, Río Negro, Argentina; MLP-CS, Museo de La Plata, Cinco Saltos collection, La Plata, Argentina; MPCA-Pv, Vertebrate Paleontology of Museo Provincial 'Carlos Ameghino,' Cipolletti, Argentina; MUCPv, Vertebrate Paleontology of Museo de la Universidad Nacional del Comahue, Neuquén, Argentina; PVL, Vertebrate Paleontology of Fundacion Miguel Lillo, Universidad Nacional de Tucumán, San Miguel de Tucumán, Argentina.

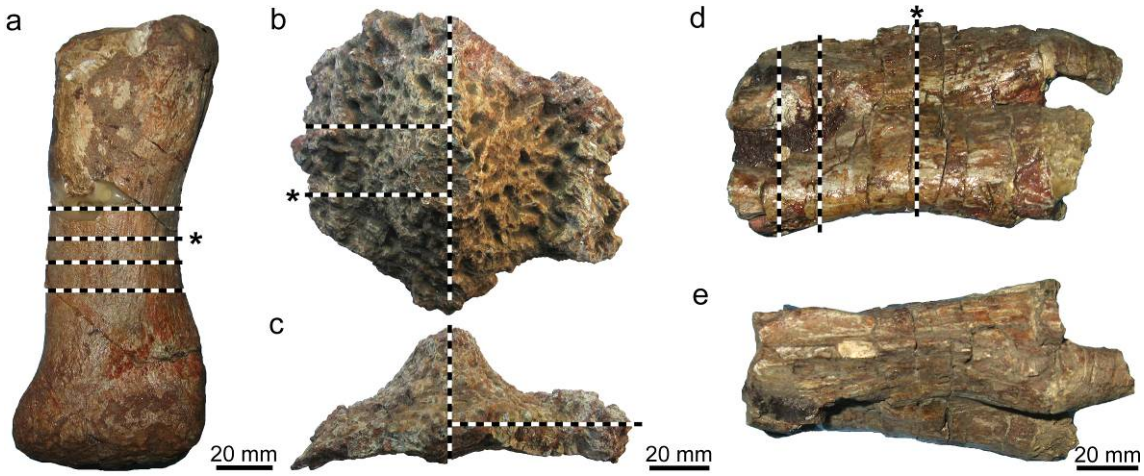

Supplementary Figure 1: Metatarsal PVL 4017-127 (**a**), osteoderm PVL 4017-113 (**b**, dorsal view; **c**, lateral view) and posterior caudal vertebra PVL 4017-140 (**d**, lateral view; **e**, dorsal view) in which unusual endosteal bone tissue was recognized. Dashed lines show the location and orientation of the thin sections. Asterisk (*) indicates the thin sections in Figures 1a, 2a and 3a.

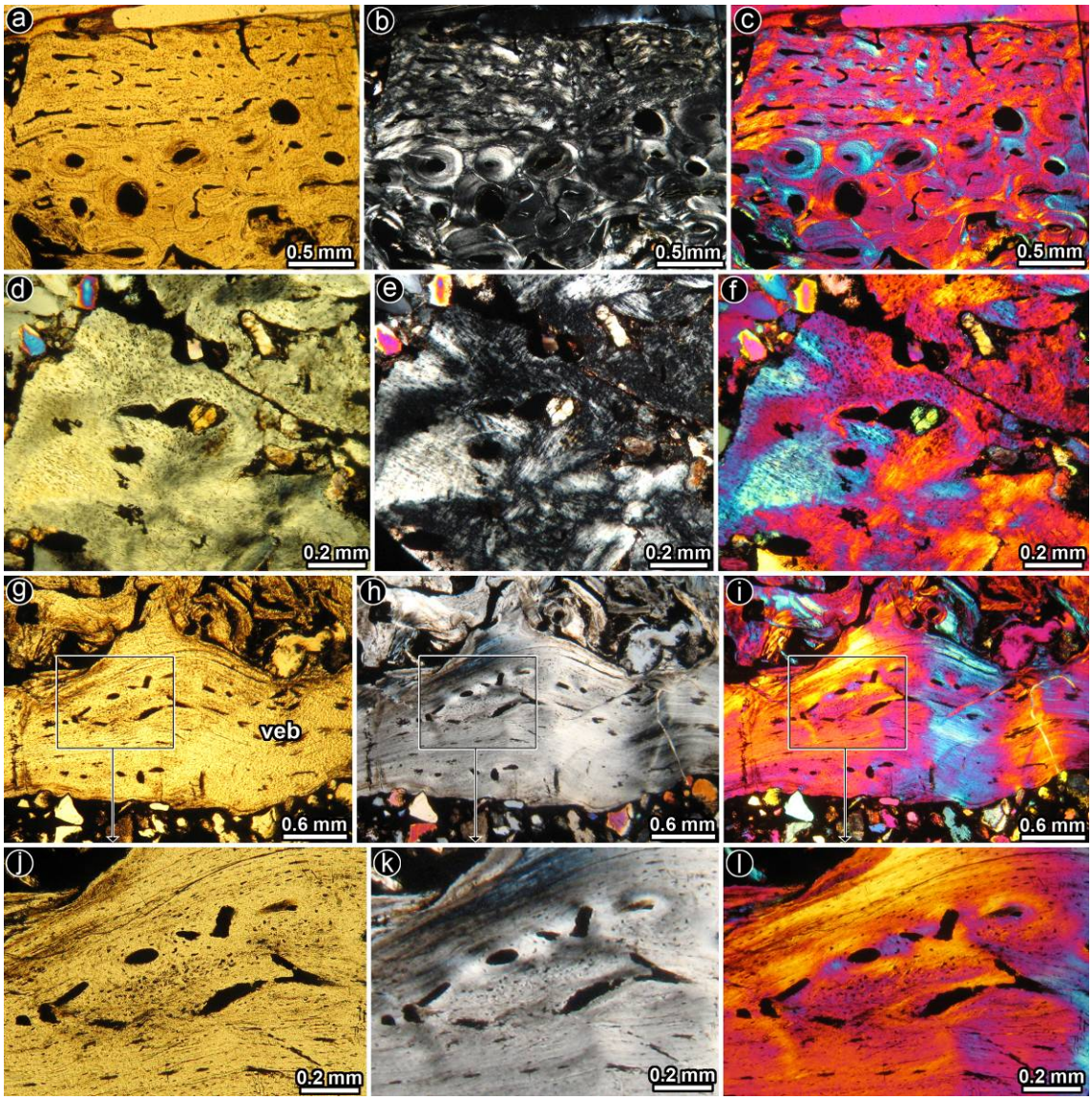

Supplementary Figure 2: Metatarsal PVL 4017-127 bone histology. **a,bc**: general view of the primary bone tissue. **d,e,f**: detailed view of the highly fibrous bone tissue at the outer cortex. **g,h,i**: general view of the vascularised endosteal bone (veb) tissue at the medullary region. **j,k,l**: detailed view of the vascularised bone tissue at the medullary region. **a,d,g,j:** normal transmitted light, **b,e,h,k:** polarized light, **c,f,i,l:** polarized light with lambda compensator.

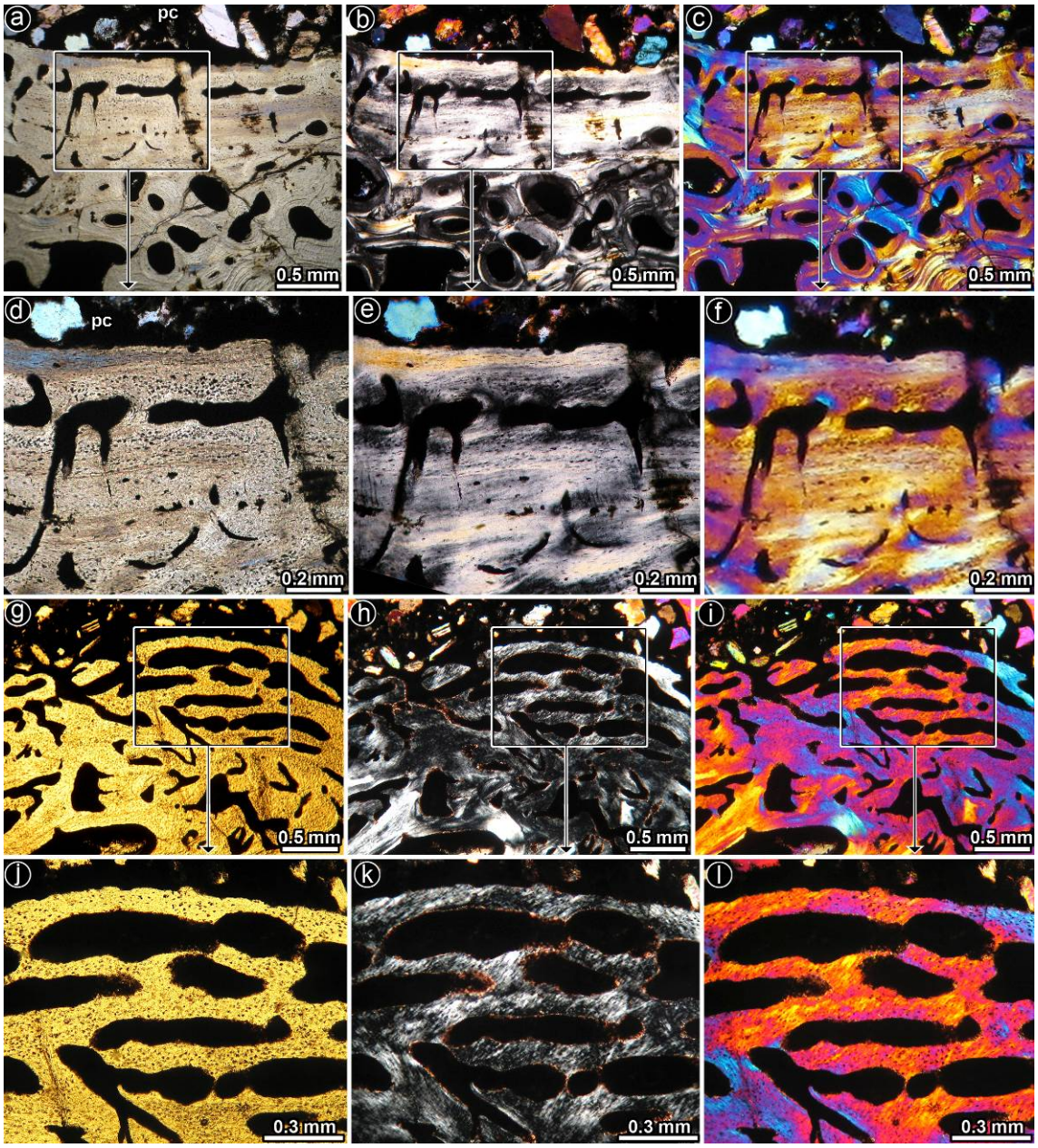

Supplementary Figure 3: bone histology of posterior caudal vertebra PVL 4017-140 (**a-f**) and osteoderm PVL 4017-113 (**g-l**). **a,b,c**: general view of the vascularised endosteal bone tissue around the pneumatic cavity. **d,e,f**: detailed view of the vascularised endosteal bone tissue around the pneumatic cavity. **g,h,i**: general view of the vascularised endosteal bone tissue around an internal cavity. **j,k,l**: detailed view of the vascularised endosteal bone tissue around an internal cavity. **a,d,g,j:** are under normal transmitted light, **b,e,h,k:** cross polarized light, **c,f,i,l:** polarized light with lambda compensator.

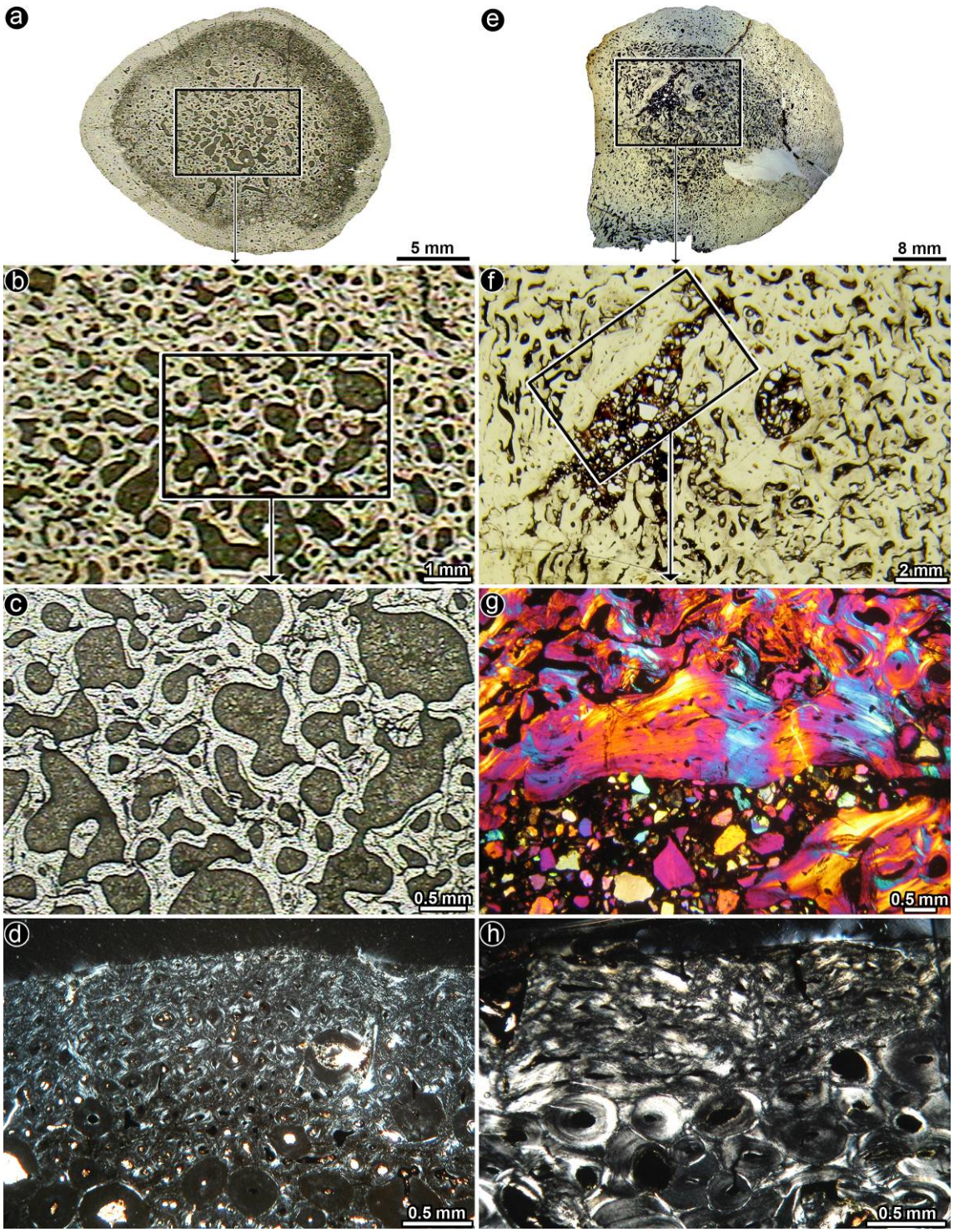

Supplementary Figure 4: Comparative histology between a titanosaur sauropod (possibly *Neuquensaurus*) MCS Pv 174/11 (**a-d**) and metatarsal PVL 4017-127 (**e-h**). **a,d**: complete transverse section at level of the midshaft. **b,f**: general view of the medullary region. **c,g**: detailed view of the medullary region. Note the presence of

vascularised endosteal bone in g. **d,h**: general view of the primary bone tissue at the outer cortex. **a,b,c,f:** are under normal transmitted light, **d,h:** cross polarized light, **g:** polarized light with lambda compensator.

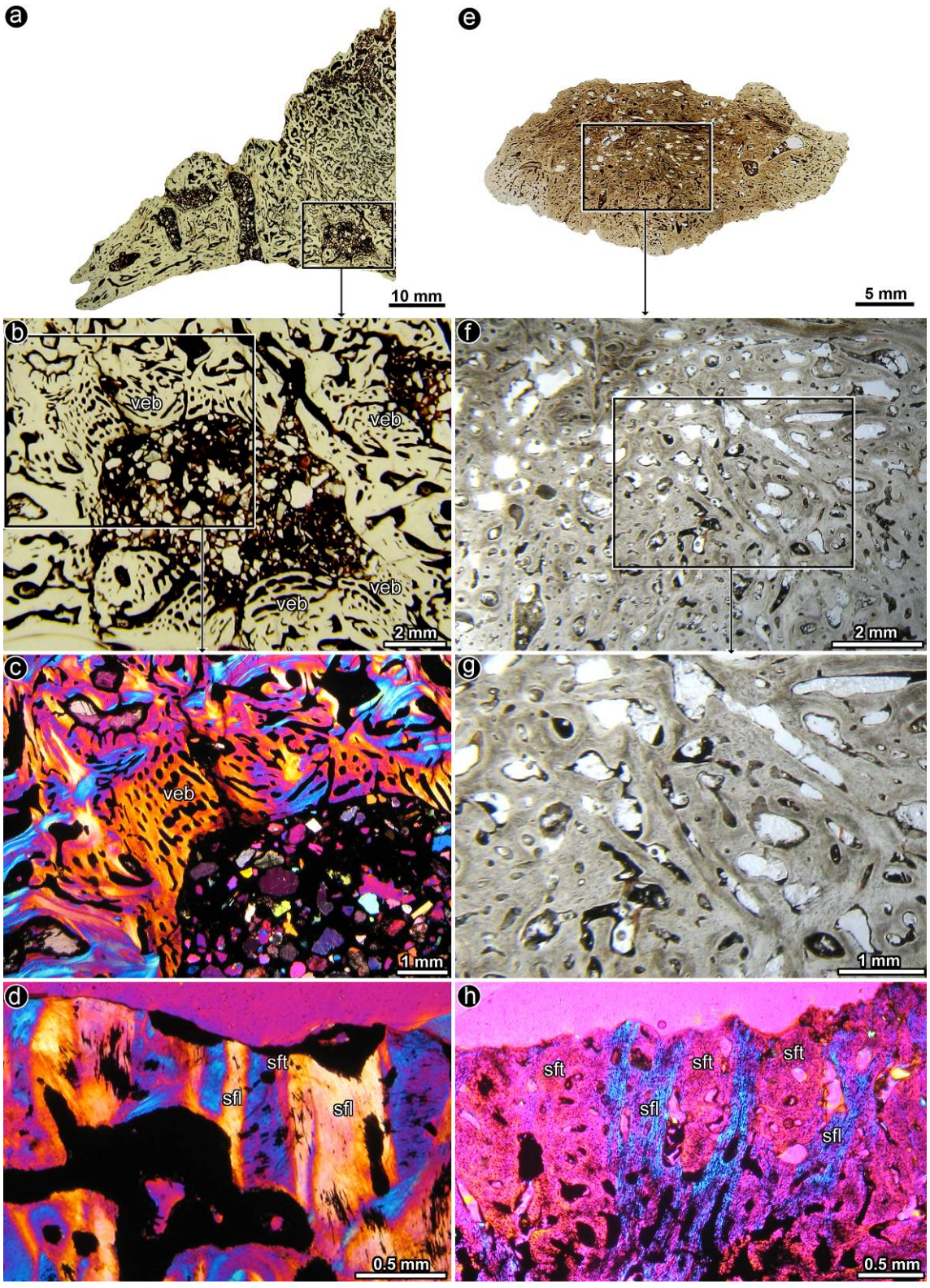

Supplementary Figure 5: Comparative histology of the osteoderm PVL 4017-113 (**a-d**) and an undetermined titanosaur sauropod MCS Pv 181 (**e-h**). **a,e**: half (**a**) and complete (**d**) cross sections. **b,f**: general view of the internal structure. Note the abundance of vascularised endosteal bone (veb) in PVL 4017-113. **c,g**: detailed view of

the internal region of the osteoderms. **d,h**: detailed view of the preserved structural fiber bundles (primary bone formed by metaplasia) in the external cortex. Structural fibers have been both transversally (sft) and longitudinally (sfl) sectioned. **a,b,e,f,g:** are under normal transmitted light; **c,d,h:** are under polarized light with lambda compensator.

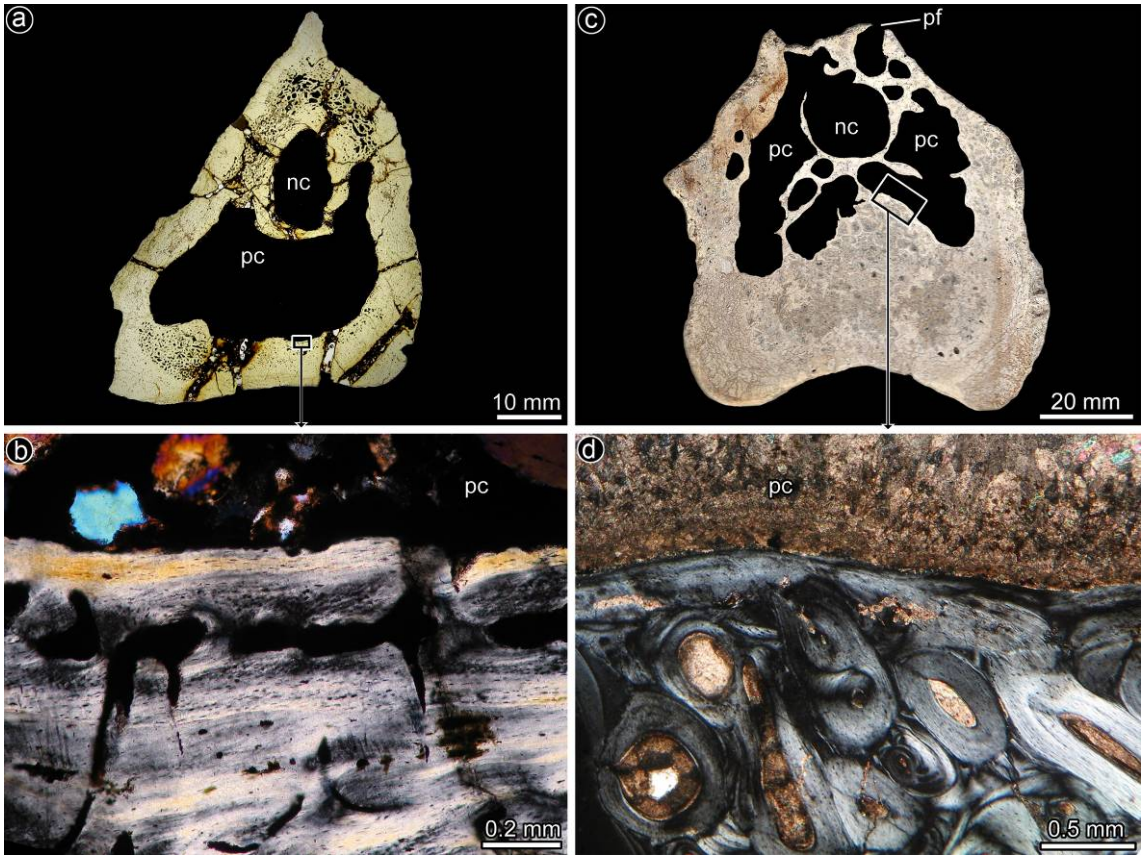

Supplementary Figure 6: Comparative histology between caudal vertebra PVL 4017-140 (**a-b**) and caudal vertebra MCS Pv 180 (**c,d**), which is assigned to *Neuquensaurus australis*. a,b: complete cross section of the vertebrae. Sediment in both neural canal (nc) and pneumatic cavities (pc) has been digitally erased. A pneumatic foramen (pf) is denoted in the neural arch of *Neuquensaurus*. **c,d**: detailed view of the bone tissue around pneumatic cavities, **a,c:** normal light, **b,d:** cross polarized light.